Theoretical Study on the Structure of the BrO Hydrates

O. Gálvez,*,† A. Zoermer, and H. Grothe

Institut für Materialchemie, Technische Universität Wien, A-1210 Vienna, Austria

Received: April 3, 2006; In Final Form: May 12, 2006

The hydrates of bromine monoxide, $BrO(H_2O)_n$, $n = 1-4$, have been studied by means of ab initio calculations at the B3LYP/aug-cc-pVTZ level of theory. These systems could be formed in the troposphere and participate in chemical reactions involved in the depletion of ozone. Several conformations are obtained and discussed for each of the hydrates mentioned. Two rather different intermolecular interactions are found, namely, conventional hydrogen bonding and Br···O associations. In contrast with a more traditional point of view in which hydrogen bonds could be assumed as the preferential interaction for the formation of these complexes, it is the Br···O association which yields the most stable conformations. Equilibrium geometries, harmonic frequencies, and relative energies have been calculated for the bromine monoxide hydrates for the first time. The theoretical binding energies indicate that the stabilization of the hydrates increases with the number of water molecules added. Cooperative effects are suggested to play a significant role in this stabilization. An analysis of relevant properties depending on the electron density in the bond critical points of the Br···O associations has been done for the first time, showing characteristic features of this interaction in comparison with the hydrogen bonds formed.

I. Introduction

During the artic polar springtime, ozone depletion occurs not only in the stratosphere but also in the marine boundary layer.[1] In these episodes, ozone drops from background concentrations of ~40 ppb down to values as low as ~0.05 ppb and frequently extends from the surface up to 1−1.5 km in altitude.[2] These events can be associated with enhanced concentration of halogen species[3,4] and are probably caused by catalytic cycles involving the radicals Br and BrO, whereas the corresponding chlorine compounds were less significant in these processes (see ref 5 and references therein). In the first instance, it was assumed that these events were only confined to the polar regions during springtime. However, recent research shows higher BrO mixing ratios also at midlatitude in coastal areas, salt deserts, and in the Dead Sea basin,[6,7] where complete boundary-layer ozone destruction is also associated with high BrO abundance.[8−10] Several processes have been suggested to produce bromine atoms and thus BrO radicals. Important sources of halogen compounds in the polar region include sea salt aerosols or sea salt deposits accumulated, e.g., on the Arctic snowpack[11] or on frost flowers.[12] Another resource are partially (poly)halogenated compounds (e.g., CH_3Br, CH_2Br_2, $CHBr_3$, CH_2BrI, etc.), which are emitted from biologic or anthropogenic sources[13] and are degraded to yield active bromine species. Recent studies revealed the importance of marine algae in the tropical oceans as a source of bromocarbons.[14,15] These sea salt and bioaerosols are lofted to the tropopause by deep convection and after decomposition provide a steady supply of bromine to the global troposphere. The catalytic mechanism leading to the so-called "tropospheric ozone hole" is well-established (see for instance refs 5,16−18); we will only outline here some relevant processes of the most important reaction cycles involving bromine species. The inorganic halogen species described above will rapidly be photolyzed to form bromine atoms, which are most likely to react with ozone

$$Br + O_3 \rightarrow BrO + O_2 \quad (1)$$

Reconversion of BrO to halogen atoms takes place by several reactions including photolysis

$$BrO + h\nu \rightarrow Br + O \quad (2)$$

In environments affected by pollution, rapid reaction with NO is another source of halogen atoms

$$BrO + NO \rightarrow Br + NO_2 \quad (3)$$

In addition to those, the self-reaction of BrO (or cross-reaction with another halogen oxide) plays an important role in the ozone destruction cycle

$$\begin{aligned} BrO + BrO &\rightarrow Br + Br + O_2 \\ &\rightarrow OBrO + Br \\ &\rightarrow Br_2 + O_2 \end{aligned} \quad (4)$$

Br_2 is assumed to photolyze rapidly into bromine atoms, but OBrO is photolyzed to yield O + BrO, so this reaction channel does not contribute to the ozone loss. Reaction 4 is the rate-limiting step of ozone destruction in this cycle I (composed by reactions 1, 2, and 4 during daytime and nonpolluted atmospheres), which has a net result of

$$2O_3 \xrightarrow{Br,\ BrO} 3O_2 \quad (5)$$

This halogen-catalyzed cycle has been identified as the prime cause for polar boundary-layer ozone destruction.[1,19] Since reaction 4 is the limiting step and thus its rate constant is proportional to $[BrO]^2$, this mechanism is ineffective at low BrO levels usually found in the free troposphere or at midlatitude

* Corresponding author. E-mail: ogalvez@iem.cfmac.csic.es.
† Current address: Departamento de Física Molecular, Instituto de Estructura de la Materia, CSIC, Serrano 123, 28006, Madrid, Spain.

10.1021/jp062048q CCC: $33.50
Published on Web 06/17/2006

TABLE 1: Equilibrium Geometries for the Two Stable Conformers of BrO·H_2O Displayed in Figure 1[a]

	OBr···OH_2 (M1)				BrO···HOH (M2)			
parameter	B3LYP[b]	MP2[b]	B3LYP[c]	MP2[c]	B3LYP[b]	MP2[b]	B3LYP[c]	MP2[c]
$r(BrO_1)$	1.734	1.707	1.761	1.749	1.727	1.693	1.751	1.737
$r(H_1\cdots O_1)$					2.049	2.037	2.015	2.078
$r(Br\cdots O_2)$	2.857	2.787	2.791	2.833				
$r(O_2H_1)$	0.962	0.962	0.963	0.960	0.967	0.966	0.967	0.963
$r(H_2O_2)$	0.962	0.962	0.963	0.960	0.961	0.961	0.961	0.959
$\theta(H_1O_1Br)$					112.5	102.0	117.4	113.0
$\theta(O_2H_1O_1)$					169.2	159.7	170.8	164.3
$\theta(O_1BrO_2)$	180.0	179.4						
$\theta(BrO_2H_1)$	120.3	125.6	124.1	124.4				
$\theta(H_2O_2H_1)$	105.7	104.8	106.1	104.2	105.4	104.4	105.3	103.8
$\tau(H_2O_2H_1O_1)$	140.4	158.5						
$-D_0$	2.54	3.48	3.33	2.85	1.58	1.70	1.88	1.32

[a] Bond lengths are given in angstroms, bond angles in degrees, and D_0 is the dissociation energy in kcal/mol (counterpoise and zero-point corrections included) of the complexes. [b] Calculated in this work. Basis set: aug-cc-pVTZ. [c] 6-311++G(d,p) in ref 26.

coastal regions. An alternative for these areas involves the formation of HOBr, and it gives rise to another cycle that produces an exponential grow of the BrO concentration, which has been summarized under the term of the so-called "bromine explosion".[20]

Ozone is a relevant greenhouse gas, a respiratory irritant, and an essential atmospheric oxidant. But the importance of the overall phenomenon described above is not limited to ozone; halogen species can have a noticeable effect on several aspects of tropospheric chemistry, e.g., they change the redox properties of the troposphere and enhance the oxidation of mercury,[21] for instance. Consequently, there are strong motivations to understand the chemistry of tropospheric bromine species. As mentioned above, BrO self-reaction is the limiting step of the ozone destruction cycle I. Recently, laboratory studies showed that ClO radicals passed over water−ice surfaces produce significant amounts of several chlorine species, including $ClClO_2$ and OClO as major reaction products.[22] The dimerization process of ClO (or BrO in reaction 4) requires the presence of a third body to stabilize the dimer before being photolyzed and decomposed into different products:

$$ClO + ClO + M \rightarrow (ClO)_2 + M$$

The authors argued that self-reaction of ClO could take place also on ice surfaces, initiated by the formation of a ClO·H_2O complex, which was proposed by ab initio calculation to exist.[23] These water complexes could play a role in enhancing the dimer formation by acting as a chaperon, as shown for the reaction of $SO_2 + H_2O$ to produce sulfuric acid.[24,25] Due to the high amount of water in the troposphere, we suggest that complexes BrO·$(H_2O)_n$, analogously to those of ClO, could also be formed, and thus, more research activities on their existence and structures could provide better insights into the bromine chemistry of the troposphere. To the best of our knowledge, and with the exception of a recent theoretical paper about the BrO·H_2O complex,[26] no previous studies have been performed for these compounds so far. In this work, high-level ab initio calculations including electron correlation and flexible basis sets have been used to directly address the geometries and energetics of the hydrates BrO·$(H_2O)_n$ from $n = 1$ to 4. The quantum methodology employed is presented in the next section, and then our results are reported and discussed. Finally, a brief section summarizes our main conclusions.

II. Computational Details

Quantum calculations were performed with the hybrid DFT method B3LYP, which consists of a mixture of Hartree−Fock (HF) exchange with Becke's three-parameters exchange functional plus the nonlocal correlation functional of Lee, Yang, and Parr. Furthermore, the MP2 method was also used in some systems in order to contrast with B3LYP calculations. As far as the size n of BrO$(H_2O)_n$ complexes increases from 1 to 4, and diffuse functions in both heavy atoms and hydrogens are necessary for proper treatment of hydrogen bonding (HB) formed, we chose the aug-cc-pVTZ basis set as a fair compromise between size and reliability. DFT calculations with a sufficiently flexible basis have been found well-suited to obtain geometries[27] and spectra[28] of bromine oxides, and systems with hydrogen-bonded structures similar to our hydrates.[29−31]

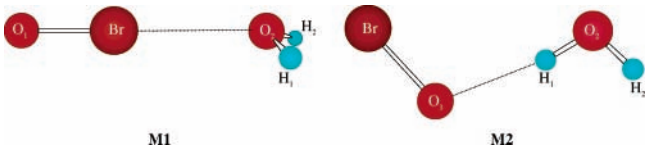

Figure 1. Plot of the B3LYP/aug-cc-pVTZ optimized geometries for the two stable conformers of BrO(H_2O).

Equilibrium geometries were fully optimized using analytic gradients without symmetry constraints. The interaction energy for every structure was then corrected for basis set superposition error (BSSE) by using the Boys−Bernardi counterpoise scheme,[32] and the zero-point energy correction (ZPEC) was also included. Geometries, frequencies, energies, and the natural population analysis (NPA)[33] were determined with the GAUSSIAN 03 package.[34] The localization and characterization of bond critical points (BCP) of the electron density according to the atoms in molecules (AIM) theory[35,36] was accomplished with the AIMPAC package.[37]

III. Results and Discussion

III.A. Geometries and Energies. The calculated geometries and zero-point vibrational energies of two conformations of BrO monohydrate are shown in Table 1. Other conformers of BrO·H_2O, for which the vibrational analysis reveals that they are not real minima because of the occurrence of imaginary frequencies, are not included in the table. As a result of the interaction between BrO and water, the complex can be formed with a hydrogen bond (H-bond; structure M2) or alternatively by a Br···O association (structure M1), as depicted in Figure 1. In all the figures shown in this article dashed lines for intermolecular bonds are drawn only if a BCP exists along the corresponding bond paths (see refs 35 and 36 for the definition of BCP). Relevant differences for the Br−O_1 and the intermolecular interaction distances are found between our B3LYP and

MP2 calculated values and those of Sun et al.,[26] which are also included in the table. A closer inspection of the origin of these differences reveals that the basis set selected by Sun et al. does not take into account polarization functions higher than "d" orbitals for bromine atoms, which are not flexible enough for a proper description of all electrons of this element. To assess our selected basis set (aug-cc-pVTZ), it is extended to aug-cc-pV5Z in a Dunning's correlated-consistent basis set framework, and to 6-311++G(3df,3pd) in the Pople's basis set description, yielding a Br−O distance in the monomer of 1.724 and 1.727 Å, respectively. These values are in good agreement with the B3LYP/aug-cc-pVTZ bond length of 1.729 Å but show large differences compared to the B3LYP/6-311++G(d,p) value of 1.756 Å of Sun et al. (see ref 26). The experimental value of 1.717 ± 0.001 Å determined by Amano et al. using microwave detection techniques[39] is also in better agreement with our predicted value than that of Sun et al. As shown in Table 1, MP2 results in shorter distances and higher interaction energy than B3LYP, especially for the conformation $OBr\cdots OH_2$. Nevertheless, both methods yield similar results and predict $OBr\cdots OH_2$ as the most stable conformer, in accord with the results of Sun et al., although the difference in energy is higher calculated by MP2 than B3LYP. The fact that HB is not the strongest interaction in this kind of systems was previously proposed by Fu et al. in their studies on $ClO\cdot H_2O$.[40] In this case, two conformations similar to those of the BrO monohydrate were obtained, and the structure $OCl\cdots OH_2$ was predicted to be around 1.6 kcal/mol more stable than the structure with HB ($ClO\cdots HOH$) at the B3LYP/6-311++G(2d,2p) level. Our calculated energies for the $ClO\cdot H_2O$ complex at B3LYP/aug-cc-pVTZ (results not shown in the tables, publication in process) predict the structure $OCl\cdots OH_2$ as the most stable too, although at only 0.70 kcal/mol with respect to the structure with HB. The fact that the structure $OCl\cdots OH_2$ was predicted as the most stable conformation, contrary to a more traditional point of view in which the HB should yield a stronger interaction, was justified by Fu et al. with the formation of two H-bonds between the water molecule and the chlorine atom. Nevertheless, our calculated distances between Cl (or Br) and the two hydrogen atoms are larger than 3.4 Å, so the formation of these H-bonds seems very improbable. In an attempt to characterize hydrogen bonds in a rigorous manner with the help of AIM theory, Popelier studied systems with well-known intermolecular H-bonds and proposed eight AIM-based criteria indicative of HB.[35,38] The first and unavoidable criterion refers to the necessary existence of a BCP of the electron density with the consistent (3, −1) topology. Neither for $OCl\cdots OH_2$ nor for $OBr\cdots OH_2$ (structure M1 in Figure 1) was a BCP found in the path between the hydrogen and the halogen atoms. Despite those findings, a (3, −1) BCP between the halogen and oxygen atom of the water molecule exists, with electron density values of 0.012 and 0.016 au for chlorine and bromine monoxide water complexes, respectively. These values are similar to those obtained for the H-bond in the M2 conformation of these compounds ($XO\cdots HOH$), which are 0.018 and 0.020 au for ClO and BrO monohydrates, respectively. Consequently, the larger stability of the conformation $OX\cdots OH_2$ (X being chlorine or bromine) must be ascribed to the association X···O, which is verified by the formation of a BCP (3, −1) in the electron density. It is also important to highlight that the conformation M2 has a smaller binding energy than that of the water dimer (−2.33 kcal/mol at the B3LYP/aug-cc-pVTZ level), indicating that a weaker H-bond is formed. Regarding the changes in the monomers when the complexes are generated, the formation of a H-bond results in a shortening of the $Br-O_1$ distance by 0.002 Å, which is small change, but it is in contrast with the increase of the B−R′ length in more conventional hydrogen bonds (represented as R−A−H···B−R′).[30] This result is quite peculiar, and it was also obtained in our calculations of the complex $ClO\cdots HOH$. More studies could be necessary to clarify the role of the halogen atoms in this effect. The distance O_2-H_1 in the water molecule increases 0.005 Å (the B3LYP/aug-cc-pVTZ geometrical values predicted for the water monomer are 0.962 Å and 105.1°), which is a typical feature of HB. With respect to the complex $OBr\cdots OH_2$, the bond $Br-O_1$ elongates by 0.005 Å, suggesting a weakening of the $Br-O_1$ bond. To explore the nature of this change, NPA charges were computed. This analysis reveals that the Br atom loses ca. 0.008 au in the formation of the complex, the same amount which is gained by the oxygen atom of the water molecule (O_2 in Figure 1). However, the atom O_1 gains around 3 times more charge (0.023 au), which results in a global transfer of ca. 0.015 au from the water molecule to the BrO radical. These changes generate an enhancement of the dipolar momentum of both the BrO and the water molecule, increasing the electrostatic interaction between Br and O_2, which entails an elongation of the bond $Br-O_1$. No relevant changes are observed for the water molecule in the formation of this conformer.

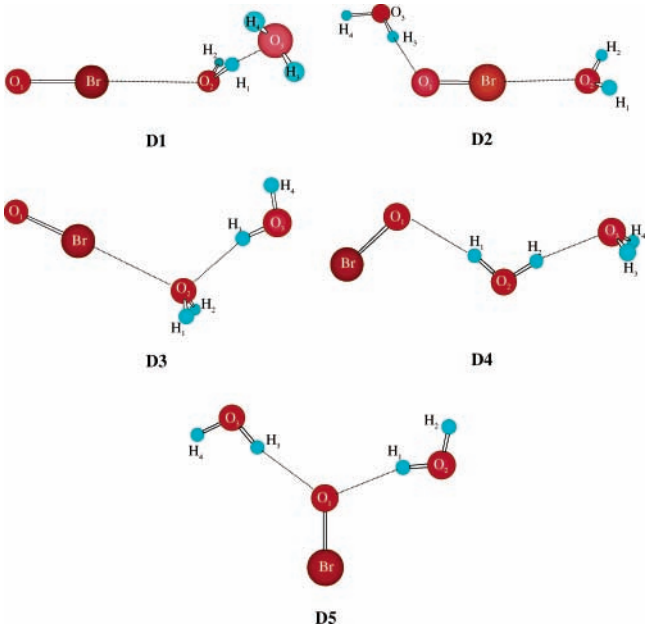

Figure 2. Equilibrium structures D1−D5 for $BrO(H_2O)_2$ complexes.

Five conformers which show real frequencies in the vibrational analysis have been found for the BrO dihydrate. Optimized geometries of these structures are shown in Figure 2, and relevant geometrical parameters found at the B3LYP/aug-cc-pVTZ level are gathered in Table 2. As a consequence of the HB interaction, and as mentioned for the conformation M2 of the monohydrate, the distance $Br-O_1$ decreases for conformers D4 and D5 with respect to that of the monomer (1.729 Å), showing a more pronounced shortenings for the latter because two H-bonds are formed. On the contrary, the distance $Br-O_1$ increases when the Br···O association takes place (conformers D1−D3), as with the monohydrate, resulting in larger increases when the Br···O distance is shorter. In the case of conformer D2, although the two interactions involved lead to opposite changes in the distance $Br-O_1$, this bond undergoes a slight elongation. This result again indicates that the association Br···O yields stronger interaction than the H-bond for these systems.

TABLE 2: Relevant Geometrical Parameters and Dissociation Energies (Counterpoise and Zero-Point Corrections Included) for the Five Conformers of $BrO(H_2O)_2$ Displayed in Figure 2[a]

parameter	D1	D2	D3	D4	D5
$r(BrO_1)$	1.738	1.732	1.733	1.727	1.725
$r(Br\cdots O)$	2.760	2.798	2.929		
$r(O_1\cdots H)$		2.000		2.132	2.093 (2.099)[b]
$r(O_{>1}\cdots H)$	1.876		2.022	1.991	
$r(OH)_{min}$	0.961	0.961	0.961	0.962	0.961
$r(OH)_{max}$	0.973	0.969	0.967	0.968	0.966
$-D_0$	6.38	4.61	4.02	3.63	2.20

[a] Bond lengths are given in angstroms, bond angles in degrees, and D_0 in kcal/mol. [b] Distance $H_3\cdots O_1$ in parentheses.

The distance Br···O in the conformers D1−D3 is shorter when the interaction energy increases in absolute value. D1 and D2 have a shorter Br···O distance than the monohydrate, but it is larger for D3, suggesting a weaker interaction, probably because the electron density of O_2 is also involved in HB. The shortest length $O_1\cdots H$ is predicted for D2, being even smaller than in the case of the monohydrate (M2), which indicates that a stronger H-bond is formed for this dihydrate. The complex D1 displays the strongest H-bonds between the water molecules, showing a distance ($r(O_{>1}\cdots H)$ in Table 2) much shorter than that of the dimer of water, 1.953 Å at the same theoretical level. In contrast, D3 has the largest distance $O_{>1}\cdots H$, which could be explained by taking into account that the electron density of the acceptor oxygen atom is also involved in the formation of the Br···O interaction, as we mentioned previously. The maximum distance O−H for all the conformers is always related to the well-known effect of the elongation of A−H bonds, which results from the formation of a hydrogen bond. Larger O−H distances are found when stronger hydrogen bonds are formed. In the case of D4 and D5, in which two H-bonds are established for each conformation, the maximum O−H distance belongs to the donor bond responsible for the strongest interaction, namely, O_2-H_2 in D4 and O_2-H_1 in D5. Considering the larger binding energies of the water dimer in comparison with those of the complex HOH···OBr makes it plausible that also for D4 a strong hydrogen bond between both water molecules is formed. Regarding the interaction energy, relevant features can be observed in Table 2. Higher $|D_0|$ are predicted when a Br···O association is formed (conformers D1−D3), in accord with the results of the monohydrate of BrO. In all the conformations depicted in Figure 2, two intermolecular interactions are found to build the dihydrates. A good estimation of their strength is the dissociation energy of the bimolecular complexes formed by the two molecules involved in the interactions, i.e., BrO·H_2O or $H_2O\cdot H_2O$ systems in this case. In conformers D1 and D2 the dissociation energy in absolute numbers is larger than the sum of the two individual intermolecular interactions. To illustrate how this effect is estimated, we will describe the procedure in more detail for conformation D1. For this complex, two intermolecular interactions similar to those in the conformation M1 of the monohydrate and in the water dimer are considered. The sum of the dissociation energies of these two bimolecular complexes yields a value of 4.87 kcal/mol, which is smaller than the dissociation energy for D1 (6.38 kcal/mol, see Table 2). The same situation is observed for the structure D2 in Figure 2, but in this case only an extra stabilization of ca. 0.5 kcal/mol is predicted. These results suggest that cooperative effects are involved in the formation of complexes D1 and D2, which are the responsible for the extra stabilization. The opposite situation is given in D3−D5, where the dissociation energies are smaller than the sum of the isolated intermolecular interactions. For these three conformers a single molecule or atom is involved twice as donor or acceptor, i.e., the central water molecule in D3 and D4 and the O_1 in D5. This situation probably causes the destabilization of these structures.

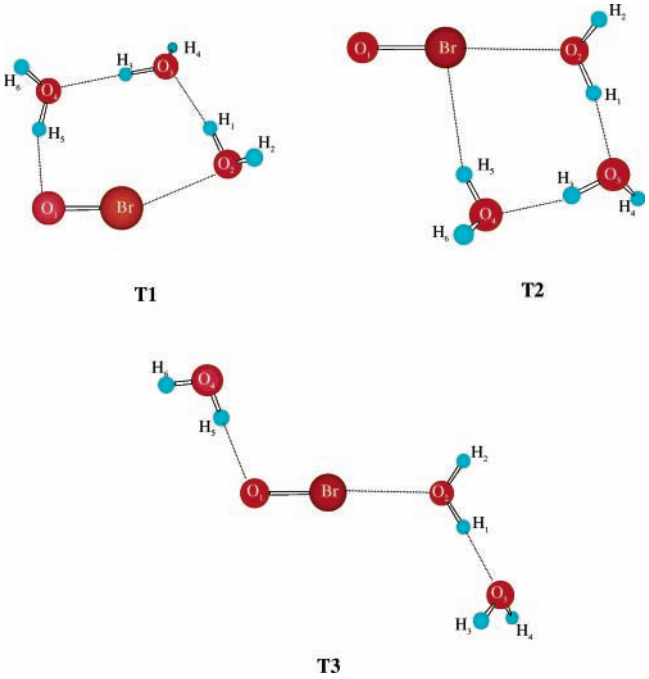

Figure 3. Equilibrium structures T1−T3 for $BrO(H_2O)_3$ complexes.

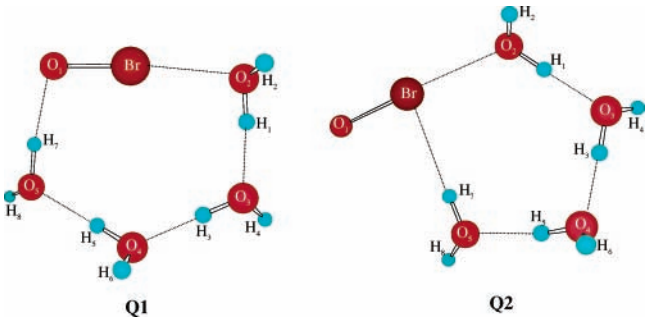

Figure 4. Equilibrium structures Q1 and Q2 for $BrO(H_2O)_4$ complexes.

To find the most stables conformations for $BrO(H_2O)_3$ and $BrO(H_2O)_4$, only those arrangement of molecules similar to the structures D1 and D2 in the dihydrates, which yield cooperative effects and large stabilization energies for these complexes, have been considered. Consequently, geometries as given in conformers D3−D5, which do not contribute an extra stabilization to these systems, are not considered for the tri- and tetrahydrates. The three stable conformers found for $BrO(H_2O)_3$ and the two most stable conformers found for $BrO(H_2O)_4$ are depicted in Figures 3 and 4, respectively, and the geometrical parameters are summarized in Table 3. According to the results found for oligomers of water,[41] cyclic structures are the most stable geometries for BrO tri- and tetrahydrates. A ring critical point (RCP) confirming the close bond arrangement formed by the corresponding bond paths is found for the T1, T2, Q1, and Q2 conformations in Figures 3 and 4. As we observed for the mono- and dihydrates, the Br···O association generates an elongation of $Br-O_1$ bond for all the complexes, which is larger when this interaction is stronger and consequently the Br···O distance is shorter. The interaction distance between BrO and water, namely, Br···O or $O_1\cdots H$, decreases with the number of water molecules added to the complex, suggesting stronger interactions and higher dissociation energies. The H-bond length between

TABLE 3: Relevant Geometrical Parameters and Dissociation Energies (Counterpoise and Zero-Point Corrections Included) for the Three Conformers of $BrO(H_2O)_3$ Displayed in Figure 3 and the Two Conformers of $BrO(H_2O)_4$ Displayed in Figure 4[a]

	$BrO(H_2O)_3$			$BrO(H_2O)_4$	
parameter	T1	T2	T3	Q1	Q2
$r(BrO_1)$	1.738	1.741	1.737	1.744	1.742
$r(Br\cdots O)$	2.747	2.691	2.702	2.610	2.657
$r(O_1\cdots H)$	2.002		1.982	1.856	
$r(Br\cdots H)$		2.682			2.592
$r(O_{>1}\cdots H)_{min}$	1.843	1.792	1.865	1.746	1.755
$r(O_{>1}\cdots H)_{max}$	1.874	1.828		1.786	1.798
$r(OH)_{min}$	0.961	0.961	0.961	0.961	0.961
$r(OH)_{max}$	0.979	0.981	0.974	0.985	0.984
$-D_0$	12.38	12.15	8.74	20.60	18.07

[a] Bond lengths are given in angstroms, bond angles in degrees, and D_0 in kcal/mol.

water molecules also decreases when the number of these in the cycle increases, like in the case of oligomers of water. Nevertheless, in BrO hydrates all the H-bond distances have different values, as a relevant difference between pure water complexes and our systems. The shortest H-bond is found for $H_1\cdots O_3$ in tri- and tetrahydrate and the longest for $H_3\cdots O_4$ in the trihydrate (structures T1 and T2) and $H_5\cdots O_3$ in the tetrahydrate. Consequently, water molecules in which the donor oxygen is also involved in a Br···O association yield the strongest H-bonds, decreasing this effect along the following intermolecular interactions forming the cycle. In summary, stronger interactions and thus more stable structures are formed when the number of water molecules increases, as can be observed by inspecting the dissociation energies in Table 3. For all the conformers drawn in Figures 3 and 4, the sum of the intermolecular interactions energies (calculated according to the procedure outlined above) is smaller than the value of D_0 shown in Table 3, revealing that cooperative effects play an important role in the formation of tri- and tetrahydrates of BrO. This extra energy amounts to 3.6 kcal/mol for T1, only 2.3 kcal/mol for T3, and as much as 9.5 kcal/mol for Q1. If we only consider the most stable structure predicted for each hydrate, this extra energy is 1.5, 3.6, and 9.5 kcal/mol for two, three, and four molecules of water, respectively. The large increase observed for the transition from three to four water molecules could be partially caused by the large decrease in the distance $O_1\cdots H$, as shown in Table 3.

III.B. Frequencies. In the present work we have carried out B3LYP calculations of the vibrational spectra for BrO and H_2O and all the conformations of BrO hydrates discussed above. For the sake of simplicity, intermolecular and other modes not relevant for the present discussion are not included in the tables, although Supporting Information of the total IR spectra of these complexes, including the intensities values, is available on request to the authors. Relevant vibrational frequencies in cm^{-1} calculated at the B3LYP/aug-cc-PVTZ level for all the conformers described above are summarized in Tables 4 and 5. Our predicted harmonic frequency for the BrO monomer is in good agreement with the experimental value of 723 cm^{-1} recorded in the gas phase.[42] This frequency is blue-shifted when the H-bond is the only interaction established between BrO and water (structures M2 and D5) and red-shifted if a Br···O association is formed, which is the case for the rest of the conformers (see Tables 4 and 5). In a recent study on the infrared spectra of several bromine oxides formed in argon matrixes, Galvez et al. identified a band at 723 cm^{-1} (10 cm^{-1} red-shifted from the BrO band), which was tentatively assigned to the M1 structure of the monohydrate.[43] Both the frequency value and the red shift with respect to the BrO band are in good agreement with our calculated values of 731 and 11 cm^{-1}, respectively. Larger red shifts are predicted when the number of water molecules increases, which corresponds to the trend shown for the $Br-O_1$ distance in the analysis of the geometries. Both the symmetric and asymmetric O−H stretching modes of the water molecules are always red-shifted, although these changes are larger when a H-bond is formed, especially for the symmetric normal mode. It could also be observed, mainly by inspection of the data in Table 5, that water molecules participating in a Br···O association undergo the largest red shifts in the stretching modes ($\nu(OH)_{HO\cdots Br}$ in the table). This fact agrees with the results presented in the previous section, where we found that these water molecules show the maximum O−H distances yielding the strongest H-bonds. The contrary situation is given for water molecules which are bonded to BrO by a H-bond ($\nu(OH)_{OH\cdots O1}$ and $\nu(OH)_{OH\cdots Br}$ in Table 5), showing the smallest red shifts in the frequency analysis as well as the weakest H-bonds, especially when the acceptor atom is bromine ($\nu(OH)_{OH\cdots Br}$ in conformation T2 and Q2). The bending O−H−O mode is always blue-shifted when a H-bond is established and stays almost unaltered (or is slightly red-shifted) if only the interaction Br···O is formed (see conformers M1 and D2 in Table 4). Larger blue shifts correspond to stronger H-bonds, increasing from $n = 1-4$ in the hydrates $BrO(H_2O)_n$.

III.C. Electron Densities. According to the results shown in the previous section, the association Br···O, and not the probably anticipated HB, is the preferential intermolecular

TABLE 4: Relevant Vibrational Frequencies (cm^{-1}) at the B3LYP/aug-cc-pVTZ Level for the BrO and Water Monomers and the Conformations of $BrO{\cdot}H_2O$ and $BrO(H_2O)_2$ Shown in Figures 1 and 2

	monomers		$BrO(H_2O)$		$BrO(H_2O)_2$				
parameter	BrO	H_2O	$OBr\cdots OH_2$ (M1)	$BrO\cdots HOH$ (M2)	D1	D2	D3	D4	D5
$\nu(BrO)$	742		731	751	721	736	730	730	758
$\nu_{as}(OH)_{nonbonded}$		3899			3887			3889	
$\nu_{sym}(OH)_{nonbonded}$		3797			3790			3790	
$\nu_{as}(OH)_{HO\cdots Br}$			3895		3862	3894	3876		
$\nu_{sym}(OH)_{HO\cdots Br}$			3794		3607	3793	3781		
$\nu_{as}(OH)_{OH\cdots O1}$				3873		3870		3804	3875 3878
$\nu_{sym}(OH)_{OH\cdots O1}$				3724		3692		3694	3746 3751
$\nu_{as}(OH)_{OH\cdots O}$							3872		
$\nu_{sym}(OH)_{OH\cdots O}$							3713		
$\delta(HOH)_{nonbonded}$		1627			1629			1629	
$\delta(HOH)_{HO\cdots Br}$			1626		1645	1625	1629		
$\delta(HOH)_{OH\cdots O1}$				1643		1650		1650	1635 1641
$\delta(HOH)_{OH\cdots O}$							1638		

TABLE 5: Relevant Vibrational Frequencies (cm^{-1}) at the B3LYP/aug-cc-pVTZ Level for the Conformations of $BrO(H_2O)_3$ and $BrO(H_2O)_3$ Shown in Figures 3 and 4

	$BrO(H_2O)_3$			$BrO(H_2O)_4$	
parameter	T1	T2	T3	Q1	Q2
ν(BrO)	726	710	729	715	709
$\nu_{as}(OH)_{HO\cdots Br}$	3858	3859	3861	3855	3860
$\nu_{sym}(OH)_{HO\cdots Br}$	3488	3452	3603	3359	3380
$\nu_{as}(OH)_{OH\cdots O1}$	3863		3869	3864	
$\nu_{sym}(OH)_{OH\cdots O1}$	3624		3679	3534	
$\nu_{as}(OH)_{OH\cdots O}$	3861	3860		3862 3862	3861 3862
$\nu_{sym}(OH)_{OH\cdots O}$	3552	3549		3433 3476	3450 3525
$\nu_{as}(OH)_{OH\cdots Br}$		3864			3863
$\nu_{sym}(OH)_{OH\cdots Br}$		3724			3712
$\delta(HOH)_{max}$	1671	1666	1653	1684	1680
$\delta(HOH)_{min}$	1641	1629	1628	1637	1631

interaction between bromine monoxide and water. Due to the central role played by HB in the properties of water, condensed matter, and biomolecular systems, enormous attention has been paid to study the nature of this interaction (the reader is referred to a few general reviews on this field[30,44−46]). For the case of the Br···O association, even though some previous studies in the literature have also shown similar interactions between halogens and oxygen as found in our systems,[23,26,40,47,48] to the best of our knowledge there is not any previous analysis exploring the nature of these interactions. In the framework of Bader's theory of atoms in molecules[35,36] the interatomic interactions can be characterized by analyzing the topological properties of the electron density, $\rho(\mathbf{r})$. Relevant features of the nature of the interaction are obtained analyzing the values of the electron density ρ_C and the Laplacian $\nabla^2\rho_C$ calculated in the BCPs. An additional analysis providing valuable information about the interactions is to explore the local energy densities at the BCP. The local expression for the virial theorem[35,36] is

$$V(\mathbf{r}) + 2G(\mathbf{r}) = \frac{1}{4}\nabla\rho^2(\mathbf{r}) \qquad (6)$$

where $V(\mathbf{r})$ and $G(\mathbf{r})$ are potential and kinetic energy densities, respectively. When integrated over the full space or over a basin Ω, the integral of $\nabla^2\rho(\mathbf{r})$ vanishes, and then the usual form of the virial theorem can be obtained. Since $G(\mathbf{r})$ is defined positive and $V(\mathbf{r})$ is defined negative, the sign of the Laplacian at the BCP also indicates which energy density dominates at $\mathbf{r}$: when $\nabla^2\rho_C > 0$, $\rho(\mathbf{r})$ is concentrated toward the nuclei and there is an excess of kinetic energy as is, for example, found in ionic and hydrogen bonds.[35,36,49] The total energy density $H(\mathbf{r}) = G(\mathbf{r}) + V(\mathbf{r})$ at the BCP, $H_C = G_C + V_C$, thus characterizes the type of bond. A negative H_C reveals the dominance of V that according to eq 6 can be viewed as the consequence of accumulating charge at the BCP. Thus, in bonds with any degree of covalent character, $|V_C| > G_C$ and $H_C < 0$. Bonds in which this condition holds but $|V_C| < 2G_C$ have been termed partially covalent, whereas $H_C > 0$ always indicates purely closed-shell interactions.[50,51] With the aim of scratching the surface of the nature of the interactions occurring in our systems, especially the Br···O association, the electron density ρ_C, the Laplacian $\nabla^2\rho_C$, and the total energy density H_C, calculated in the BCPs have been analyzed. The values of ρ_C and H_C both in the monomers and in the intermolecular interactions of the most stable conformations of the BrO hydrates are gathered in Table 6. The BCP in the $Br-O_1$ bond is situated approximately in the midpoint between both atoms, contrary to a classical O−H bond in which it is located very close to the hydrogen atom (its position is at around 20% for a conventional H-bond, expressed as a percentage of the total distance measured from the hydrogen atom). The fact that the BCP is far from both atoms could account for the low value of ρ_C in the Br−O bond; nevertheless, it also suggests a weak interaction between these atoms (e.g., the calculated value for a more stable bond like in the oxygen molecule is 0.5393 au). For the conformation M2 only an intermolecular hydrogen bond is formed, resulting a slightly higher electron density in the BCP of the $Br-O_1$ bond. For the rest of the conformations, a Br···O association in addition to the HB is present and the ρ_C in the $Br-O_1$ bond of the complexes is lower than the value in the BrO monomer, decreasing when more water molecules are added, in accord with both the elongation of the $Br-O_1$ bond and the red shift of the corresponding stretching mode. Although the changes in the electron density are consistent with the structural modification of the $Br-O_1$ bonds, the effects are indeed very small, changing the values of ρ_C less than 0.008 au. The same trend is observed for the ρ_C in the covalent bond O_2-H_1 of the water molecule; however, the changes of ρ_C are 1 order of magnitude higher than those for the $Br-O_1$ bond. The electron densities of the intermolecular interactions are usually 1 order of magnitude lower than those of conventional covalent bonds. The Br···O association has values of ρ_C similar to those of the hydrogen bonds, as mentioned. This value increases when more water molecules participate in the hydrate complexes, yielding stronger Br···O associations, which agrees with the short

TABLE 6: Electron Density ρ_C and Total Energy Density H_C in au Calculated in Relevant Interatomic BCPs for the BrO and Water Monomers and the Most Stable Conformations of the BrO Hydrates Depicted in Figures 1−4

			$BrO\cdot H_2O$		$BrO(H_2O)_2$	$BrO(H_2O)_3$		$BrO(H_2O)_4$	
parameter	BrO	H_2O	M1	M2	D1	T1	T2	Q1	Q2
					electron density, ρ_C				
$r(BrO_1)$	0.2078		0.2058	0.2082	0.2040	0.2032	0.2031	0.2005	0.2027
$r(O_2H_1)$		0.3710	0.3699	0.3643	0.3552	0.3482	0.3456	0.3407	0.3419
$r(Br\cdots O)$			0.0155		0.0198	0.0215	0.0233	0.0281	0.0246
$r(O_1\cdots H)$				0.0199		0.0232		0.0328	
$r(O_{>1}\cdots H)_{max}$					0.0299	0.0328	0.0376	0.0416	0.0406
$r(O_{>1}\cdots H)_{min}$						0.0299	0.0336	0.0372	0.0358
$r(Br\cdots H)$							0.0117		0.0134
					total energy density, H_C				
$r(BrO_1)$	−0.1735		−0.1714	−0.174 6	−0.1690	−0.168 2	−0.1677	−0.164 6	−0.167 2
$r(O_2H_1)$		−0.7411	−0.7440	−0.737 1	−0.7275	−0.713 1	−0.7086	−0.699 6	−0.702 8
$r(Br\cdots O)$			0.0024		0.0024	0.0022	0.0023	0.0018	0.0023
$r(O_1\cdots H)$				0.0008		0.0000		−0.003 9	
$r(O_{>1}\cdots H)_{max}$					−0.0025	−0.003 8	−0.0060	−0.008 1	−0.007 7
$r(O_{>1}\cdots H)_{min}$						−0.002 7	−0.0039	−0.006 0	−0.005 1
$r(Br\cdots H)$							0.0006		0.0002

distance calculated. The same situation is found for the H-bonds formed, including those involving Br as the acceptor atom. In the analysis of the interaction energy of the complexes previously described, cooperative effects were suggested to play an important role in the extra stabilization found in some of the conformations, e.g., the structures D1 and D2 with respect to structures D3−D5. For the complexes which show this cooperative effects, we found that the sum of the ρ_C values calculated in the intermolecular bonds (Br···O and O···H in Table 6) are higher than the sum of the individual intermolecular interactions calculated in the corresponding bimolecular complexes (results not shown). Consequently, the electron density reflects the existence of these cooperative effects which were previously observed in the analysis of the interaction energy.

The Laplacian of $\rho(\mathbf{r})$ is a sensitive probe to identify subtle spatial changes of charge concentrations not evident in the $\rho(\mathbf{r})$ itself. If $\nabla^2\rho(\mathbf{r}) < 0$ at a given point, $\rho(\mathbf{r})$ is locally concentrated there, and conversely, if $\nabla^2\rho(\mathbf{r}) > 0$, then $\rho(\mathbf{r})$ is locally depleted. A negative $\nabla^2\rho_C$ occurs in all shared electron (covalent) interactions, while a positive $\nabla^2\rho_C$ reveals a depletion of electron charge along the bond path, which is a common feature of all closed-shell (electrostatic) interactions.[35] For the sake of clarity, values of $\nabla^2\rho_C$ are not included in Table 6, although their signs are discussed next. The covalent O−H bonds have $\nabla^2\rho(\mathbf{r}) < 0$, whereas the Br−$O_1$ bond yields very small but positive values of $\nabla^2\rho(\mathbf{r})$, which is a typical feature of a closed-shell interaction according to the AIM theory. The fact that $\nabla^2\rho_C > 0$ for this bond suggests a weak interaction between these atoms, which agrees with the high instability of this radical. All the intermolecular interactions, i.e., HB and Br···O associations, show the expected positive values of the Laplacian.

The H_C values for the relevant bonds of the BrO hydrates are also included in Table 6. Covalent interactions such as O−H bonds show negative values of the H_C. Despite the positive values of $\nabla^2\rho_C$, the bond Br−O_1 yields negative values of H_C for all the compounds, so although it has been classified as a closed-shell interaction, a partially covalent character and a shared electron character is expected for this bond. When more molecules of water are added, the H-bonds formed (O_1···H, $O_{>1}$···H, and Br···H in Table 6) are stronger and negative values of the H_C are found for higher hydrates. Nevertheless, the Br···O association shows positive values of H_C for all the compounds studied. Although the values and especially the signs of these parameters give us a preliminary idea about the nature of the Br···O association, a deeper understanding of both the Br···O association itself and the origin of the cooperative effects shown in these hydrates should be a matter of further studies which go beyond the scope of this article.

IV. Conclusions

We have studied the hydrates of bromine monoxide BrO-$(H_2O)_n$, $n = 1-4$, by means of ab initio calculations. These systems could participate in the cycles of reactions responsible for ozone depletion in the troposphere, mainly in the arctic vortex during springtime. Our main goal in exploring these compounds is to elucidate their structure and vibrational spectrum for the first time and also to gain insight into the nature of the intermolecular interactions, i.e., HB and especially the Br···O associations formed. Our predicted bond length and vibrational frequency for the monomer BrO are in good agreement with the experimental values available for this molecule. No previous information on BrO hydrates exist with the only exception of BrO·H_2O, of which the structure calculated ab initio has been recently reported in the literature, although the selected basis set was not flexible enough to give a good representation of this complex. The B3LYP method yields results similar to those provided by MP2 calculations for the monomers and BrO·H_2O, showing the reliability of our calculations to address the larger complexes. An HB or a Br···O association could be formed in the complex BrO·H_2O, but the Br···O association yields a conformation around 1 kcal/mol more stable than the H-bonded one. This situation generally persists when the number of water molecules increases. The difference in energy between the most stable conformers which contain Br···O associations and those with only hydrogen bonds is getting larger when more molecules of water are added. Cyclic structures are found for the global minimum geometries of BrO-$(H_2O)_3$ and BrO$(H_2O)_4$, and an RCP is found in the topological analysis of $\rho(\mathbf{r})$, in concordance with the results for oligomers of water. When more water molecules are added, the dissociation energy of the hydrates could not be accounted by for the sum of the intermolecular interactions formed, and cooperative effects are suggested to be involved in these further stabilizations. The calculated frequencies for the hydrates predict blue shifts in the Br−O stretching mode when a hydrogen bond is formed and red shifts when a Br···O association is established. The O−H stretching modes of the water molecules also undergo red shifts in any case when the hydrates are formed, although these shifts are larger when the molecule is additionally participating in a Br···O association. All these shifts are larger when more water molecules are forming the complex. The analysis of the values of the electron density, the Laplacian of $\rho(\mathbf{r})$, and the total density energy in the BCPs reveals features relevant for the interactions formed. The Br−O bond shows small values of ρ_C, positive values of $\nabla^2\rho_C$, and negative values of H_C revealing a partially covalent character for this bond. When the distance H···O in the H-bonds is lower than ca. 1.9 Å, H_C shows negative values, although $\nabla^2\rho_C$ takes positive values in all cases. Despite the fact that the Br···O association yields compounds of higher stability than the hydrogen bond, the analysis of the $\nabla^2\rho_C$ and H_C for this interaction reveals positive values for these parameters, suggesting that the electrostatic interactions are the main cause of this interaction.

Acknowledgment. This research was supported by the European Union, INTAS Project 03-51-5698. O.G. acknowledges financial support from the Spanish Ministerio de Educación y Ciencia, MEC. We thank Dr. Luis Fernández Pacios for his help in the preparation of this manuscript.

References and Notes

(1) Barrie, L. A.; Bottenheim, J. W.; Schnell, R. C.; Crutzen, P. J.; Rasmussen, R. A. *Nature* **1998**, *224*, 134.

(2) Bottenheim, J. W.; Fuentes, J. D.; Tarasick, D. W.; Anlauf, K. G. *Atmos. Environ.* **2002**, *36*, 2535.

(3) Haussmann, M.; Platt, U. *J. Geophys. Res.* **1994**, *99*, 25399.

(4) Impey, G. A.; Shepson, P. B.; Hastie, D. R.; Barrie, L. A.; Anlauf, K. G. *J. Geophys. Res.* **1997**, *102*, 16005.

(5) Platt, U.; Hönninger, G. *Chemosphere* **2003**, *52*, 325.

(6) Hebestreit, K.; Stutz, J.; Rosen, D.; Matveev, V.; Peleg, M.; Luria, M.; Platt, U. *Science* **1999**, *283*, 55.

(7) Matveev, V.; Peleg, M.; Rosen, D.; Tov-Alper, D. S.; Stutz, J.; Hebestreit, K.; Platt, U.; Blake, D.; Luria, M. *J. Geophys. Res.* **2001**, *106*, 10375.

(8) Weissflog, L.; Elansky, N.; Puntz, E.; Krueger, G.; Lange, C. A.; Lisitzina, L.; Pfennigsdorff, A. *Atmos. Environ.* **2004**, *38*, 4197.

(9) Ferlemann, F.; Camy-Peyret, C.; Harder, H.; Fitzenberger, R.; Hawat, T.; Osterkamp, H.; Perner, D.; Platt, U.; Schneider, M.; Vradelis, P.; Pfeilsticke, K. *Geophys. Res. Lett.* **1998**, *25*, 3847.

(10) Fitzenberger, R.; Bösch, H.; Camy-Peyret, C.; Chipperfield, M. P.; Harder, H.; Platt, U.; Sinnhuber, B.-M.; Wagner, T.; Pfeilsticker, K. *Geophys. Res. Lett.* **2000**, *27*, 2921.

(11) Foster, K.; Plastridge, R.; Bottenhein, J.; Shepson, P.; Finlayson-Pitts, B.; Spicer, C. W. *Science* **2001**, *291*, 471.
(12) Kaleschke, L.; Richter, A.; Burrows, J.; Afe, O.; Heygster, G.; Notholt, J.; Rankin, A. M.; Roscoe, H. K.; Hollwedel, J.; Wagner, T.; Jacobi, H. W. *Geophys. Res. Lett.* **2004**, *31*, L16114, 1.
(13) Cicerone, R. J. *Rev. Geophys. Space Phys.* **1981**, *19*, 123.
(14) Salawitch, R. J. *Nature* **2006**, *439*, 275.
(15) Yang, X.; Cox, R. A.; Warwick, N. J.; Pyle, J. A.; Carver, G. D.; O'Connor, F. M.; Savage, N. H. *J. Geophys. Res.* **2005**, *110*, D23311.
(16) Wayne, R. P.; Poulet, G.; Biggs, P.; Burrows, J. P.; Cox, R. A.; Crutzen, P. J.; Haymann, G. D.; Jenkin, M. E.; LeBras, G.; Moortgat, G. K.; Platt, U.; Schindler, R. N. *Atmos. Environ.* **1995**, *29*, 2675.
(17) Lary, D. J.; Chipperfield, M. P.; Toumi, R.; Lenton, T. *J. Geophys. Res.* **1996**, *101*, 1489.
(18) Platt, U.; Moortgat, G. K. *J. Atmos. Chem.* **1999**, *34*, 1.
(19) Barrie, L. A.; Platt, U. *Tellus* **1997**, *49B*, 450.
(20) Platt, U.; Jassen, C. *Faraday Discuss.* **1996**, *100*, 175.
(21) Lu, J. Y.; Schroeder, W. H.; Barrie, L. A.; Steffen, A.; Welch, H. E.; Martin, K.; Lockhart, W. L.; Hunt, R. V.; Boila, G.; Ritchter, A. *Geophys. Res. Lett.* **2001**, *28*, 3219.
(22) McKeachie, J. R.; Appel, M. F.; Kirchner, U.; Schindler, R. N.; Benter, Th. *J. Phys. Chem. B* **2004**, *108*, 16786.
(23) Francisco, J. S.; Sander, S. P. *J. Am. Chem. Soc.* **1995**, *117*, 9917.
(24) Moroukuma, K.; Moroukuma, C. *J. Am. Chem. Soc.* **1994**, *116*, 10316.
(25) Kolb, C. E.; Jayne, J. T.; Worsnop, D. R.; Molina, M. J.; Meads, R. F.; Viggiano, A. A. *J. Am. Chem. Soc.* **1994**, *116*, 10314.
(26) Sun, Q.; Li, Z.; Zeng, X. Q.; Ge, M. F.; Wang, D. X. *Chin. J. Chem.* **2005**, *23*, 483.
(27) Guha, S.; Francisco, J. S. *J. Phys. Chem. A* **1997**, *101*, 5347.
(28) Guha, S.; Francisco, J. S. *J. Phys. Chem. A* **1998**, *102*, 6702.
(29) Gálvez, O.; Gómez, P. C.; Pacios, L. F. *J. Chem. Phys.* **2003**, *118*, 4878.
(30) Gálvez, O.; Gómez, P. C.; Pacios, L. F. *J. Chem. Phys.* **2001**, *115*, 11166.
(31) Schrems, O.; Sennikov, P. G.; Ignatov, S. K. *ChemPhysChem* **2005**, *6*, 392.
(32) Boys, S. F.; Bernardi, F. *Mol. Phys.* **1970**, *19*, 553.
(33) (a) Reed, A. E.; Weinstock, R. B.; Weinhold, F. *J. Chem. Phys.* **1985**, *83*, 735. (b) Reed, A. E.; Weinhold, F.; Curtiss, L. A. *Chem. Rev.* **1988**, *88*, 899.
(34) Frisch, M. J.; Trucks, G. W.; Schlegel, H. B.; Scuseria, G. E.; Robb, M. A.; Cheeseman, J. R.; Montgomery, J. A., Jr.; Vreven, T.; Kudin, K. N.; Burant, J. C.; Millam, J. M.; Iyengar, S. S.; Tomasi, J.; Barone, V.; Mennucci, B.; Cossi, M.; Scalmani, G.; Rega, N.; Petersson, G. A.; Nakatsuji, H.; Hada, M.; Ehara, M.; Toyota, K.; Fukuda, R.; Hasegawa, J.; Ishida, M.; Nakajima, T.; Honda, Y.; Kitao, O.; Nakai, H.; Klene, M.; Li, X.; Knox, J. E.; Hratchian, H. P.; Cross, J. B.; Adamo, C.; Jaramillo, J.; Gomperts, R.; Stratmann, R. E.; Yazyev, O.; Austin, A. J.; Cammi, R.; Pomelli, C.; Ochterski, J. W.; Ayala, P. Y.; Morokuma, K.; Voth, G. A.; Salvador, P.; Dannenberg, J. J.; Zakrzewski, V. G.; Dapprich, S.; Daniels, A. D.; Strain, M. C.; Farkas, O.; Malick, D. K.; Rabuck, A. D.; Raghavachari, K.; Foresman, J. B.; Ortiz, J. V.; Cui, Q.; Baboul, A. G.; Clifford, S.; Cioslowski, J.; Stefanov, B. B.; Liu, G.; Liashenko, A.; Piskorz, P.; Komaromi, I.; Martin, R. L.; Fox, D. J.; Keith, T.; Al-Laham, M. A.; Peng, C. Y.; Nanayakkara, A.; Challacombe, M.; Gill, P. M. W.; Johnson, B.; Chen, W.; Wong, M. W.; Gonzalez, C.; Pople, J. A. *GAUSSIAN 03*; Gaussian Inc.: Wallingford, CT, 2004.
(35) Bader, R. F. W. *Atoms in Molecules: A Quantum Theory*; Claderon: Oxford, 1990.
(36) Popelier, P. L. A. *Atoms in Molecules: An Introduction*; Prentice-Hall: Harlow, 2000.
(37) Biegler-Konig, F. W.; Bader, R. F. W.; Tang, T. H. *J. Comput. Chem.* **1982**, *3*, 317.
(38) (a) Koch, U.; Popelier, P. L. A. *J. Phys. Chem.* **1995**, *99*, 9747. (b) Popelier, P. L. A. *J. Phys. Chem. A* **1998**, *102*, 1873.
(39) Amano, T.; Yoshinaga, A.; Hirota, E. *J. Mol. Spectrosc.* **1972**, *44* (33), 594.
(40) Fu, H.; Zhou, Z.; Zhou, X. *Chem. Phys. Lett.* **2003**, *382*, 466.
(41) Diri, K.; Myshakin, E. M.; Jordan, K. D. *J. Phys. Chem. A* **2005**, *109*, 4005.
(42) Drouin, B. J.; Miller, C. E.; Müller, H. S. P.; Cohen, E. A. *J. Mol. Spectrosc.* **2001**, *205*, 128.
(43) Gálvez, O.; Zoermer, A.; Loewenschuss, A.; Grothe, H. *J. Phys. Chem. A*, in press.
(44) Jeffrey, G. *An Introduction to Hydrogen Bonding*; Oxford University Press: New York, 1997.
(45) Scheiner, S. *Hydrogen Bonding: A Theoretical Perspective*; Oxford University Press: New York, 1997.
(46) Desiraju, G.; Steiner, T. *The Weak Hydrogen Bond. In Structural Chemistry; Biology*; Oxford University Press: Oxford, 1999.
(47) Beukes, J. A.; D'Anna, B.; Bakkeb, V.; Nielsen, C. J. *Phys. Chem. Chem. Phys.* **2000**, *2*, 4049.
(48) Wang, L.; Liu, J.-Y.; Li, Z.-D.; Sun, C.-C. *Chem. Phys. Lett.* **2005**, *411*, 225.
(49) Carroll, T.; Bader, R. F. W. *Mol. Phys.* **1988**, *65*, 695.
(50) Arnold, W. D.; Oldfield, E. *J. Am. Chem. Soc.* **2000**, *122*, 12835.
(51) Jenkins, S.; Morrison, I. *Chem. Phys. Lett.* **2000**, *317*, 97.